Available online at www.sciencedirect.com
SCIENCE DIRECT®
Finite Elements in Analysis and Design 42 (2005) 50–70
FINITE ELEMENTS IN ANALYSIS AND DESIGN
www.elsevier.com/locate/finel

Structural dynamics modification via reorientation of modification elements

Eui-Il Jung[a], Youn-Sik Park[a], K.C. Park[b,*]

[a] *Department of Mechanical Engineering, Center for Noise and Vibration Control, Korea Advanced Institute of Science and Technology, Daejon 305-701, Korea*
[b] *Department of Aerospace Engineering Sciences, Center for Aerospace Structure, University of Colorado, Boulder, CO 80309, USA*

Received 5 October 2004; received in revised form 18 April 2005; accepted 1 May 2005
Available online 19 July 2005

Abstract

The present paper describes a structural dynamics modification (SDM) method, labeled as *layout reorientation method* by attaching and reorienting modification structural elements on the baseline structure. The present method is distinctly different from existing fixed layout pattern SDM methods which utilize a fixed modification layout pattern and vary material properties or geometrical dimensions. The present method determines both the position and orientation of the modification structural elements to be placed on the basic structure. A challenge in the present method is how to resolve grid non-matching problem between the baseline structure and modification elements, for which a virtual interface frame concept between the nodes of the baseline and modification structures is employed. The potential of the present SDM method is demonstrated via numerical examples.
© 2005 Elsevier B.V. All rights reserved.

Keywords: Structural modification; Optimization; Structural dynamics

1. Introduction

Structural dynamics modification (SDM) is widely used to change natural frequencies and/or mode shapes by adding and deleting auxiliary members for improving the dynamic response of a target structure. Most of the existing SDM approaches deal with the material property or the size of structures for a

* Corresponding author.
E-mail addresses: yspark@kaist.ac.kr (Y.-S. Park), kcpark@colorado.edu (K.C. Park).

0168-874X/$ - see front matter © 2005 Elsevier B.V. All rights reserved.
doi:10.1016/j.finel.2005.05.004

given structural layout [1–3]. In the present paper it is assumed that the base structure has been already designed via a variety of methods and procedures including topology optimization [4]. While topology optimization for vibration problems has been investigated by several investigators (see, e.g., [5] and others cited in [4, p. 310]), structural dynamics modifications are distinctly different from the problems posed by topology design for vibration problems. First, its application is primarily aimed at *modifying* (more precisely perturbing) existing structures for the next generation design cycle. Second, it may provide an alternative method for obviating the so-called non-smoothness of eigenvalues discussed in [6], among others.

In the present paper, an attempt is made to place the modification structural elements on the baseline structure by determining their translational positions and the rotational orientations, thus effectively realizing the redesign of the layout of modifying structures for improving the natural frequencies of the resulting structure. A motivation for the present approach is our belief that employing the layout variations of modifying structural elements could accomplish more easily the stated design goal than by employing the optimization of the material properties and the size variations of a fixed-layout system. A similar approach was proposed by Twu and Choi [7,8] who developed a continuum-based configuration design sensitivity using a material derivative idea, and applied it to beam and truss optimization. In order for their idea to be applied to discretized FE models, the discrete model needs to be re-meshed for every new design obtained from each iteration step of optimization process. Thus, the computational cost can be high to implement in real engineering problems with finite elements models.

In the present study, a modular substructure coupling concept is introduced in SDM when attaching auxiliary structures to the baseline structure. Thus, the optimization problem is reduced to finding the attaching position of auxiliary structures. In a typical substructural synthesis, each of the substructure is modeled separately and assembled into a whole structure without having to generate a new mesh. However, node mismatch problem can occur on the interfacing surface of the substructures. This is particularly true in layout optimization, for which the attaching structural members move continuously on the baseline structure such that interface nodes usually do not match. Recently, several investigators addressed non-matching interface problems. Farhat and Geradin [9] used a Lagrange multiplier function which represents the interface tractions for gluing non-matching nodes in application of component mode synthesis. Park and Felippa [10] presented a continuum-based variational principle for the formulation of the discrete governing equations of partitioned structural systems. The interface is treated by an interface frame and the localized Lagrange multipliers. Park et al. [11] presented a frame nodal displacement criterion to carry out the frame discretization into piecewise linear elements. It should be noted that in the interface frame concept, the discrete models of both the baseline structure and the attaching elements are preserved, and the task of remeshing is delegated to the discretization of the frame only.

In this paper the interface frame concept is adopted for an effective layout optimization. The interfacing displacements of modifying substructures are constrained to those of the baseline structure during optimization process, thus circumventing remeshing. In the optimization process, of several methods to calculate eigenvalues of the combined whole structure (e.g., see: [12–15]), we adopt a determinant search method. Since the attaching structure moves continuously on the baseline structure, sensitivities to determine the moving direction are essential for each optimization iteration. The eigenvalue sensitivities of the attaching structure to the moving direction of the attaching members are formulated using the Simpson method [14]. Finally, the optimal structural modification is obtained by iteratively carrying out the eigenvalue sensitivities and eigenvalue reanalysis. Numerical examples demonstrate the basic features and performance of the proposed SDM approach.

2. Partitioned equations for structures having non-matching interface nodes

Consider a structure composed of three substructures as shown in Fig. 1. The bottom substructure is the baseline structure and the upper two substructures represent modification structures introduced to alter the natural frequencies of the baseline structure. When synthesizing the substructures, we would like to preserve the discrete nodes of the three substructures. Imagine now one or both of the modification substructures move with respect to the baseline structure so that the interface nodal pattern is altered. One way to preserve the original nodal patterns of the three substructures is to introduce an interface frame along the interface surface, to which the substructures are brought to be connected, instead of direct connection one another. It can be shown that there exists a unique constraint condition between the interface displacements of substructures and those of the frame. Specifically, the interface constraint condition between the substructure and the frame (not the interfacing substructure) can be expressed as

$$\mathbf{u}_{\Gamma_s} - \mathbf{u}_f = 0, \tag{1}$$

where $\mathbf{u}_{\Gamma_s}$ is the interface displacement of substructure s and $\mathbf{u}_f$ is the frame displacement that *matches* with the substructural interface displacement.

Observe that each substructure is connected to the interface frame, *not* to the adjacent substructure, which is labeled as *localized constraint conditions* in Park and Felippa [10]. Thus, when the above localized constraint condition is augmented to the completely free virtual work of each substructures, the following constrained Hamilton's principle is obtained:

$$\delta \int (T - V + \Pi_\lambda)\,\mathrm{d}t = 0, \quad T = \sum_{s=0}^{n_s-1} T_s, \quad V = \sum_{s=0}^{n_s-1} V_s, \quad \Pi_\lambda = \sum_{s=0}^{n_s-1} \int_{\Gamma_s} \lambda_s (\mathbf{u}_s - \mathbf{u}_f)\,\mathrm{d}\Gamma_s \tag{2}$$

in which T_s and V_s are the kinetic and potential energies of substructure s; $\mathbf{u}_s$, $\mathbf{u}_f$, n_s and Γ_s denote the substructural displacement, the interface frame displacement, the number of substructures and the boundary of substructures, respectively; $\mathrm{d}\Gamma_s$ is used for the boundary integral; and, λ_s is the localized Lagrange multiplier associated to the sth substructure, effectively forcing the interface constraint condition (1) for each substructure. It should be noted that the method of classical Lagrange multipliers connects one substructural interface directly to that of its adjacent substructures.

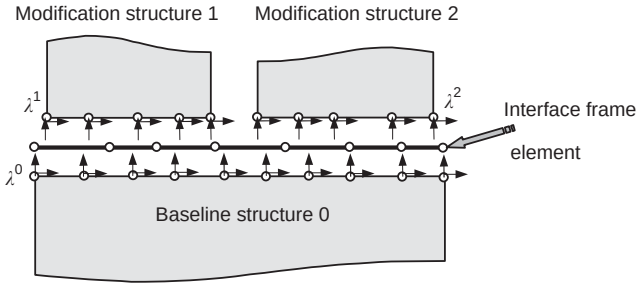

Fig. 1. Substructure synthesis employing the method of localized Lagrange multipliers.

First, we discretize $\mathbf{u}_s$, λ_s and $\mathbf{u}_f$ with suitable shape functions:

$$u_s = \mathbf{N}_u^{(s)}\mathbf{u}_s, \quad \lambda_s = \mathbf{N}_\lambda^{(s)}\boldsymbol{\lambda}_s, \quad \text{and} \quad u_f = \mathbf{N}_f\mathbf{u}_f, \tag{3}$$

where $\mathbf{N}_u^{(s)}$, $\mathbf{N}_\lambda^{(s)}$ and $\mathbf{N}_f$ are shape functions of the displacement, the localized Lagrange multiplier and the interface frame displacement, respectively, and $\mathbf{u}_s$, $\boldsymbol{\lambda}_s$ and $\mathbf{u}_f$ are nodal vectors. Thus, when Eq. (2) is discretized via (3), the following discrete Hamilton's equation is obtained:

$$\delta \int \sum_{s=0}^{n_s-1} \left(\frac{1}{2}\dot{\mathbf{u}}_s^{\mathrm{T}}\mathbf{M}_s\dot{\mathbf{u}}_s - \frac{1}{2}\mathbf{u}_s^{\mathrm{T}}\mathbf{K}_s\mathbf{u}_s + \mathbf{f}_s^{\mathrm{T}}\mathbf{u}_s + \boldsymbol{\lambda}_s^{\mathrm{T}}\mathbf{B}_s\mathbf{u}_s - \boldsymbol{\lambda}_s^{\mathrm{T}}\mathbf{C}_{fs}\mathbf{u}_f \right) \mathrm{d}t = 0 \tag{4}$$

in which

$$\mathbf{B}_s = \int_{\Omega_s} \mathbf{N}_\lambda^{(s)^{\mathrm{T}}}\mathbf{N}_u^{(s)}\,\mathrm{d}\Omega_s, \quad \mathbf{C}_{fs} = \int_{\Gamma_s} \mathbf{N}_\lambda^{(s)^{\mathrm{T}}}\mathbf{N}_f\,\mathrm{d}\Gamma_s, \tag{5}$$

$\mathbf{M}_s$, $\mathbf{K}_s$, $\mathbf{f}_s$, $\mathbf{B}_s$ and $\mathbf{C}_{fs}$, are the mass matrix, stiffness matrix of the sth substructure, external force on sth substructure, interface Boolean matrix and interpolation matrix, respectively. Usually the shape functions of the localized Lagrange multipliers are chosen as delta functions located at substructure nodes. Then, the connection matrix, $\mathbf{B}_s$, becomes a Boolean matrix with 0 or 1 entries, which indicates a nodal point connected to the neighboring substructure.

From the discrete variational equation (4), the partitioned domain-by-domain equations for each substructure and its force and displacement compatibility conditions can be derived as

$$\begin{aligned}
&\delta\mathbf{u}_s: \quad \mathbf{M}_s\ddot{\mathbf{u}}_s + \mathbf{K}_s\mathbf{u}_s = \mathbf{f}_s + \mathbf{B}_s^{\mathrm{T}}\boldsymbol{\lambda}_s \qquad s = 0, 1, \ldots, (n_s - 1),\\
&\delta\boldsymbol{\lambda}_s: \quad \mathbf{B}_s\mathbf{u}_s - \mathbf{C}_{fs}\mathbf{u}_f = 0, \qquad s = 0, 1, \ldots, (n_s - 1),\\
&\delta\mathbf{u}_f: \quad \sum_{s=0}^{n_s-1} \mathbf{C}_{fs}^{\mathrm{T}}\boldsymbol{\lambda}_s = 0.
\end{aligned} \tag{6}$$

The partitioned governing equations for the entire structure can be rewritten by stacking up the above relations as follows:

$$\begin{aligned}
&\begin{bmatrix} \mathbf{M} & 0 & 0 \\ 0 & 0 & 0 \\ 0 & 0 & 0 \end{bmatrix} \begin{bmatrix} \ddot{\mathbf{u}} \\ \ddot{\boldsymbol{\lambda}} \\ \ddot{\mathbf{u}}_f \end{bmatrix} + \begin{bmatrix} \mathbf{K} & -\mathbf{B}^{\mathrm{T}} & 0 \\ -\mathbf{B} & 0 & \mathbf{C}_f \\ 0 & -\mathbf{C}_f^{\mathrm{T}} & 0 \end{bmatrix} \begin{bmatrix} \mathbf{u} \\ \boldsymbol{\lambda} \\ \mathbf{u}_f \end{bmatrix} = \begin{bmatrix} \mathbf{f} \\ 0 \\ 0 \end{bmatrix},\\
&\mathbf{u}^{\mathrm{T}} = [\mathbf{u}_0\ \mathbf{u}_1\ .\ \mathbf{u}_{\mathbf{n}_s-1}]^{\mathrm{T}}\\
&\boldsymbol{\lambda}^{\mathrm{T}} = [\boldsymbol{\lambda}_0\ \boldsymbol{\lambda}_1\ .\ \lambda_{n_s-1}]^{\mathrm{T}}.
\end{aligned} \tag{7}$$

We will employ the preceding partitioned equations of motion for synthesizing structural modification. To this end, by assuming periodic motions at frequency ω and with $\mathbf{f} = 0$, the frequency equation for the synthesized whole structure is obtained from the partitioned governing equation (7):

$$\begin{bmatrix} \mathbf{D}(\boldsymbol{\omega}) & -\mathbf{B}^{\mathrm{T}} & 0 \\ -\mathbf{B} & 0 & \mathbf{C}_f \\ 0 & \mathbf{C}_f^{\mathrm{T}} & 0 \end{bmatrix} \begin{bmatrix} \mathbf{u} \\ \lambda \\ \mathbf{u}_f \end{bmatrix} = \begin{bmatrix} 0 \\ 0 \\ 0 \end{bmatrix}, \quad \mathbf{D}(\boldsymbol{\omega}) = \mathbf{K} - \omega^2\mathbf{M} = \mathbf{H}(\boldsymbol{\omega})^{-1}, \tag{8}$$

where $\mathbf{D}(\boldsymbol{\omega})$ is the substructure-by-substructure dynamic stiffness. It should be noted that ω in the above equation represents the frequencies of the assembled total system equations, not the substructural frequencies.

Since the number of structural nodes is usually larger than that of the interface nodes, it is preferable to reduce the size of Eq. (8). First, we obtain $\mathbf{u}(\boldsymbol{\omega})$ from the first row of Eq. (8) as

$$\mathbf{u}(\boldsymbol{\omega}) = \mathbf{H}(\boldsymbol{\omega})\mathbf{B}^{\mathrm{T}}\boldsymbol{\lambda}(\boldsymbol{\omega}). \tag{9}$$

Substituting this into the second and third rows of Eq. (8) leads to a reduced equation of motion:

$$\begin{bmatrix} -\mathbf{H}(\boldsymbol{\omega})_{bb} & \mathbf{C}_f \\ \mathbf{C}_f^{\mathrm{T}} & 0 \end{bmatrix} \begin{bmatrix} \lambda \\ \mathbf{u}_f \end{bmatrix} = \mathbf{E}(\boldsymbol{\omega}) \begin{bmatrix} \boldsymbol{\lambda} \\ \mathbf{u}_f \end{bmatrix} = 0, \quad \mathbf{H}(\boldsymbol{\omega})_{bb} = \mathbf{B}\mathbf{H}(\boldsymbol{\omega})\mathbf{B}^{\mathrm{T}}, \tag{10}$$

where subscript, b, denotes the interface degrees of freedom which are much smaller compared to the total degrees of freedom. The matrix is block diagonal in terms of the interface degrees of freedom of each substructure. To have a non-trivial solution, the determinant of matrix $\mathbf{E}(\boldsymbol{\omega})$ must be equal to zero, which leads to the characteristic equation. There are many methods to solve for eigenvalues yielded by the characteristic equation. In the present study, a method suggested by Yee and Tsuei [13] will be adopted as they are known to alleviate numerical instabilities, which solves the following equation:

$$det(\mathbf{E}(\boldsymbol{\omega})) = \Pi_{i=0}^{n_s-1}\Pi_{j=1}^{n_m}(\omega_{ij}^2 - \omega^2) = 0, \tag{11}$$

where ω_{ij} is the jth natural frequency of the ith substructure and n_m is the number of modes of the ith substructure in the frequency range of interest. After obtaining the rth natural frequency ω_r, the eigenvector corresponding to $[\boldsymbol{\lambda}^{\mathrm{T}}, \mathbf{u}_f^{\mathrm{T}}]$ can be calculated when needed.

In Eq. (10), the number of degrees of freedom can be drastically reduced to the number of the interface degree of freedom. This means that calculating the limited number of frequency response functions at the interfacing points would enable one to obtain the natural frequencies of the synthesized structure. Experimentally measured frequency response function at the interfacing points can also be used instead of those from the FE model.

3. Placement of modification members by employing partitioned equations of motion

Our modification problem can be stated as follows:

$$\max\left[\omega_{\min} = \min_{i=1}^{N} \omega_i\right] \tag{12}$$

that is s.t.

$$\begin{aligned} &(\mathbf{K} - \omega_i^2\mathbf{M})\Phi_i = 0, \quad i = 1, \ldots, N, \\ &(x_m, y_m) \in D, \quad 0 \leqslant \theta_m \leqslant \pi, \quad m = 1, \ldots, n_m, \\ &\sum \mathbf{m}_m \leqslant M_m, \end{aligned} \tag{13}$$

where $(\mathbf{K}, \mathbf{M})$ are the stiffness and mass of the combined base and modification beams, (x_m, y_m) denotes the center of the modification beam, θ_m is the angular orientation of the modification beam, D is the permissible domain for the modification beam placement, m_m is the mass of each modification beam, M_m is the total allowable modification beams, and subscripts (N, n_m) designate the total degrees of freedom of the modified structures and the total number of modification beams, respectively.

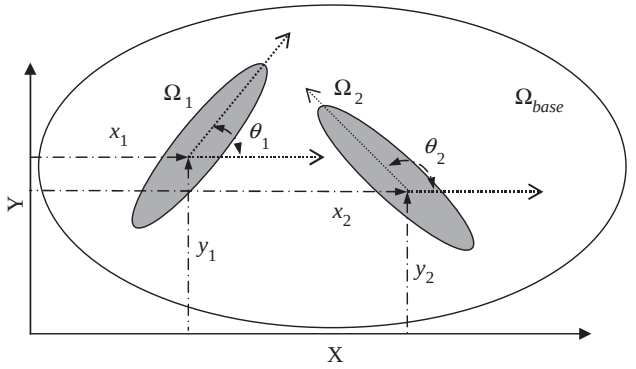

Fig. 2. Reorientation design variables $g = [x_1, y_1, \theta_1, x_2, y_2, \theta_2]^{\mathrm{T}}$.

To modify effectively the natural frequencies of the baseline structure, an eigenvalue sensitivity formulation with respect to the design variables is needed. Eigenvalue sensitivities are very helpful to guide the preferable direction and location of the modification members to be placed. Simpson [14] formulated an eigenvalue sensitivity equation for a coupled system using the derivatives of mass and stiffness matrices with respect to the design variables. In this work, the design variables to be used in the eigenvalue sensitivity are the position and orientation of the modification members, viz., (x, y) and θ as shown in Fig. 2. The design variables can be expressed as $g_i = [x_i, y_i, \theta_i]^{\mathrm{T}}$ if we take two design modification beams where subscripts i denotes the ith modification member. For the rth natural frequency ω_r of the synthesized structure, pre- and post-multiplying Eq. (10) by $[\boldsymbol{\lambda}^{\mathrm{T}}, \mathbf{u}_f^{\mathrm{T}}]$ result in

$$-\boldsymbol{\lambda}^{\mathrm{T}}\mathbf{H}_{bb}(\boldsymbol{\omega}_r)\boldsymbol{\lambda} + 2\boldsymbol{\lambda}^{\mathrm{T}}\mathbf{C}_f(\boldsymbol{\omega}_r)\mathbf{u}_f = 0. \tag{14}$$

It is assumed that the number of the interfacing boundary nodes is kept unchanged, but the nodal position moves as the position design variable, (x, y) and the rotational design variable θ are changed. Differentiating Eq. (11) with respect to the ith position design variable $\mathbf{g}_i$ gives

$$-\boldsymbol{\lambda}^{\mathrm{T}}\frac{\mathrm{d}\mathbf{H}_{bb}(\boldsymbol{\omega}_r)}{\mathrm{d}g_i}\boldsymbol{\lambda} + 2\boldsymbol{\lambda}^{\mathrm{T}}\frac{\mathrm{d}\mathbf{C}_f(\boldsymbol{\omega}_r)}{\mathrm{d}g_i}\mathbf{u}_f = 0. \tag{15}$$

Since changes in the design variables affect both the natural frequency and the frequency response function (FRF), the derivative of the interface FRF is expressed as

$$\frac{\mathrm{d}\mathbf{H}_{bb}(\boldsymbol{\omega}_r)}{\mathrm{d}g_i} = \frac{\partial\mathbf{H}_{bb}(\boldsymbol{\omega}_r)}{\partial g_i} + \frac{\partial\mathbf{H}_{bb}(\boldsymbol{\omega}_r)}{\partial\omega_r}\frac{\partial\omega_r}{\partial g_i}. \tag{16}$$

From Eqs. (15) and (16), the desired eigenvalue sensitivity can be written as follows:

$$\frac{\partial\omega_r}{\partial g_i} = \frac{\sum_{s=0}^{n_s-1}(-\boldsymbol{\lambda}_s^{\mathrm{T}}(\partial\mathbf{H}_{bb}^{(s)}(\boldsymbol{\omega}_r)/\partial g_i)\boldsymbol{\lambda}_s + 2\boldsymbol{\lambda}_s^{\mathrm{T}}(\mathrm{d}\mathbf{C}_f(\boldsymbol{\omega}_r)/\mathrm{d}g_i)\mathbf{u}_f)}{\sum_{s=0}^{n_s-1}(\boldsymbol{\lambda}_s^{\mathrm{T}}(\partial\mathbf{H}_{bb}^{(s)}(\boldsymbol{\omega}_r)/\partial\omega_r)\boldsymbol{\lambda}_s)}. \tag{17}$$

In Eq. (16), the interface FRF variation and the interpolation derivative are needed to obtain the eigenvalue sensitivity expression (17). Since the interface FRF is not affected by the position design

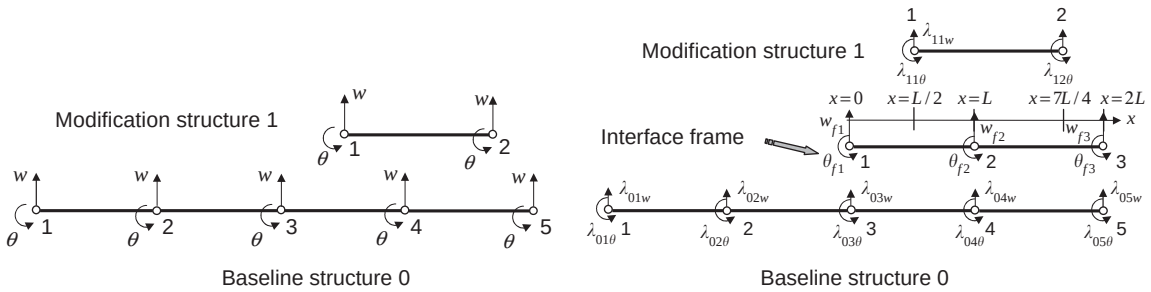

Fig. 3. Frame and localized Lagrange multipliers for modeling of non-matching substructural interfaces.

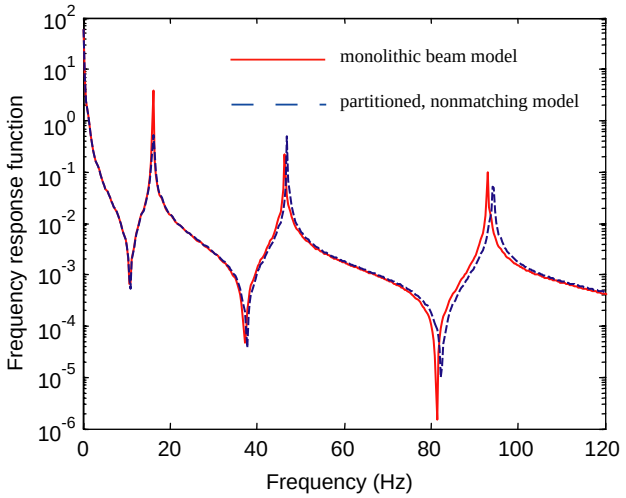

Fig. 4. Accuracy of partitioned non-matching beam model.

variable (x_s, y_s) but by the rotational design variable (θ_s), the interface FRF can be expressed as

$$\mathbf{H}_{bb}^{(s)}(\boldsymbol{\omega}_r, \boldsymbol{\theta}_s) = \mathbf{T}(\boldsymbol{\theta}_s)^{\mathrm{T}} \mathbf{H}_{bb}^{(s)}(\boldsymbol{\omega}_r, \mathbf{0}) \mathbf{T}(\boldsymbol{\theta}_s), \tag{18}$$

where $\mathbf{T}(\boldsymbol{\theta}_s)$ is the coordinate transformation matrix due to the rotation θ_s. Therefore, the derivative of the interface FRF is obtained by differentiating Eq. (18) as

$$\frac{\mathrm{d}\mathbf{H}_{bb}^{(s)}(\boldsymbol{\omega}_r, \boldsymbol{\theta}_s)}{\mathrm{d}\theta_s} = \frac{\mathrm{d}\mathbf{T}(\boldsymbol{\theta}_s)^{\mathrm{T}}}{\mathrm{d}\theta_s} \mathbf{H}_{bb}^{(s)}(\boldsymbol{\omega}_r, 0) \mathbf{T}(\boldsymbol{\theta}_s) + \mathbf{T}(\boldsymbol{\theta}_s)^{\mathrm{T}} \mathbf{H}_{bb}^{(s)}(\boldsymbol{\omega}_r, 0) \frac{\mathrm{d}\mathbf{T}(\boldsymbol{\theta}_s)}{\mathrm{d}\theta_s}. \tag{19}$$

The derivative of the frame node matrix $\mathbf{C}_{fs}$ with respect to the design variables $\mathbf{g}_s$ of substructure Ω_s is expressed as

$$\frac{\mathrm{d}\mathbf{C}_{fs}}{\mathrm{d}g_s} = \int_{\Gamma_s} \mathbf{N}_{\boldsymbol{\lambda}}^{(s)\mathrm{T}} \frac{\mathrm{d}\mathbf{N}_f(\xi, \eta)}{\mathrm{d}g_s} \mathrm{d}\Gamma_s, \quad g_s = (x_s, y_s, \theta_s), \tag{20}$$

Table 1
Convergence of natural frequencies for non-matching beam cases

	Matched FEM	Non-matched FEM	Difference (%)
1st natural freq.	16.08	16.17	0.5
2nd natural freq.	46.39	46.98	1.3
3rd natural freq.	93.02	93.90	1.3
4th natural freq.	158.20	166.38	5.0

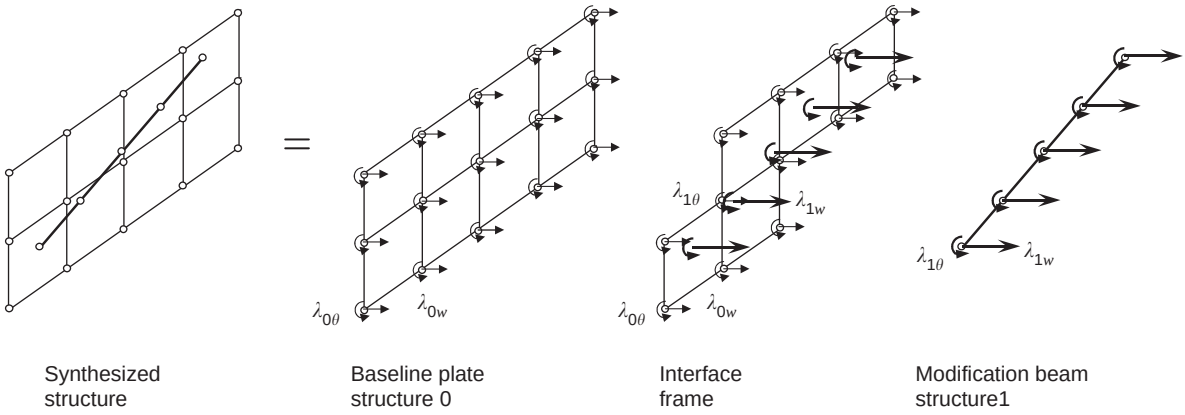

Fig. 5. Construction of frame for non-matching interface between plate and modifying beam.

where the shape function derivatives can be expressed by invoking the standard finite element procedure as

$$\begin{bmatrix} \dfrac{\mathrm{d}\mathbf{N}_f(\xi,\eta)}{\mathrm{d}x_s} \\ \dfrac{\mathrm{d}\mathbf{N}_f(\xi,\eta)}{\mathrm{d}x_s} \end{bmatrix} = \mathbf{J}_s^{-1} \begin{bmatrix} \dfrac{\partial\mathbf{N}_f(\xi,\eta)}{\partial\xi} \\ \dfrac{\partial\mathbf{N}_f(\xi,\eta)}{\partial\eta} \end{bmatrix}, \quad \mathbf{J}_s = \begin{bmatrix} x_{s,\xi} & y_{s,\xi} \\ x_{s,\eta} & y_{s,\eta} \end{bmatrix},$$

$$\frac{\mathrm{d}\mathbf{N}_f(\xi,\eta)}{\mathrm{d}\theta_s} = [x_{s,\theta}\ \ y_{s,\theta}]\ \mathbf{J}_s^{-1} \begin{bmatrix} \dfrac{\partial\mathbf{N}_f(\xi,\eta)}{\partial\xi} \\ \dfrac{\partial\mathbf{N}_f(\xi,\eta)}{\partial\eta} \end{bmatrix}. \tag{21}$$

From Eqs. (19) to (21), the eigenvalue sensitivity vector with respect to the position design variables of the sth modification substructure Ω_s (17) can be written as

$$\begin{bmatrix} \dfrac{\partial\omega_r}{\partial x_s} \\ \dfrac{\partial\omega_r}{\partial y_s} \\ \dfrac{\partial\omega_r}{\partial\theta_s} \end{bmatrix} = \frac{[\mathbf{A}]}{\sum_{s=0}^{n_s-1} \left(\boldsymbol{\lambda}_s^{\mathrm{T}} \dfrac{\partial\mathbf{H}_{bb}^{(s)}(\omega_r)}{\partial\omega_r} \boldsymbol{\lambda}_s \right)},$$

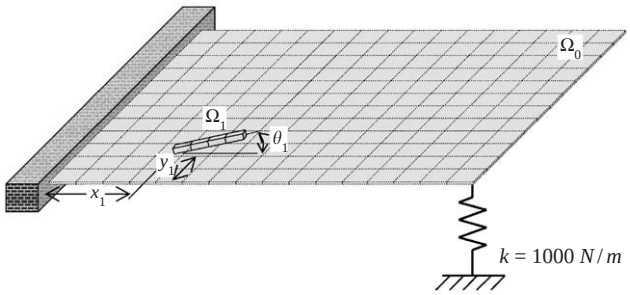

Fig. 6. Present layout reorientation design variables of beam stiffener (cantilevered plate).

$$[\mathbf{A}] = \begin{bmatrix} 0 \\ 0 \\ -\boldsymbol{\lambda}_s^{\mathrm{T}} \dfrac{\mathrm{d}\mathbf{H}_{bb}^{(s)}(\omega_r, \boldsymbol{\theta}_s)}{\partial \theta_s} \boldsymbol{\lambda}_s \end{bmatrix} + 2 \begin{bmatrix} \boldsymbol{\lambda}_s^{\mathrm{T}} & 0 & 0 \\ 0 & \boldsymbol{\lambda}_s^{\mathrm{T}} & 0 \\ 0 & 0 & \boldsymbol{\lambda}_s^{\mathrm{T}} \end{bmatrix} \begin{bmatrix} 1 & 0 \\ 0 & 1 \\ -l_s \sin\theta_s & l_s \cos\theta_s \end{bmatrix} \times \mathbf{J}_s^{-1} \begin{bmatrix} \dfrac{\partial \mathbf{N}_f(\xi,\eta)}{\partial \xi} \\ \dfrac{\partial \mathbf{N}_f(\xi,\eta)}{\partial \eta} \end{bmatrix}. \tag{22}$$

4. Example problems

4.1. A beam problem

In implementing the design sensitivity vector, the construction of the frame node matrix $\mathbf{C}_f$ is required. As the frame nodes are a new concept in connection with design optimization, its construction will first be demonstrated by using a simple beam structure. The beam has modulus of elasticity of 200 Gpa, density of 7800 kg/m^3, height of 2 mm, and width of 10 mm. As shown in Fig. 3, the baseline structure has four beam elements and the modification structure has one beam element. Since each node of a beam element has two variables: the vertical displacement w and the rotational slope θ (not to be confused with the rotational variable of the modification member orientation), it is natural to have the vertical displacement w_f and the rotational slope θ_f for the interface frame as well. Therefore, the shape function of the interface frame takes the form of Hermitian cubic interpolations as follows:

$$\begin{bmatrix} w_f \\ \theta_f \end{bmatrix} = \begin{bmatrix} \left(1-\dfrac{3x^2}{L^2}+\dfrac{2x^3}{L^3}\right) & \left(x-\dfrac{2x^2}{L}+\dfrac{x^3}{L^2}\right) & \left(\dfrac{3x^2}{L^2}-\dfrac{2x^3}{L^3}\right) & \left(\dfrac{-x^2}{L}+\dfrac{x^3}{L^2}\right) \\ \left(\dfrac{-6x}{L^2}+\dfrac{6x^2}{L^3}\right) & \left(1-\dfrac{4x}{L}+\dfrac{3x^2}{L^2}\right) & \left(\dfrac{6x}{L^2}-\dfrac{6x^2}{L^3}\right) & \left(\dfrac{-2x}{L}+\dfrac{3x^2}{L^2}\right) \end{bmatrix} \begin{bmatrix} w_{f1} \\ \theta_{f1} \\ w_{f2} \\ \theta_{f2} \end{bmatrix}. \tag{23}$$

Here, $L=0.2$ m becomes the length of the interface frame element. Note that the interface frame nodes are collocated with the baseline structure nodes. Since the localized Lagrange multipliers are also collocated at substructure nodes, they are shown in Fig. 3 accordingly. In this case the frame node matrix $\mathbf{C}_f$ is evaluated from the interface frame shape function at the appropriate interface position as follows.

For the baseline structure (denoted by subscript 0) and the frame (denoted by subscript *f*), one finds the following constraint:

$$\begin{aligned}
&\mathbf{B}_0\,\mathbf{u}_0 - \mathbf{C}_{f0}\,\mathbf{u}_f = 0,\\
&\mathbf{B}_0 = \begin{bmatrix} 0 & 0 & 1 & 0 & 0 & 0 & 0 & 0\\ 0 & 0 & 0 & 1 & 0 & 0 & 0 & 0\\ 0 & 0 & 0 & 0 & 1 & 0 & 0 & 0\\ 0 & 0 & 0 & 0 & 0 & 1 & 0 & 0\\ 0 & 0 & 0 & 0 & 0 & 0 & 1 & 0\\ 0 & 0 & 0 & 0 & 0 & 0 & 0 & 1 \end{bmatrix}, \quad \mathbf{C}_{f0} = \mathbf{I}(6,6),\\
&\mathbf{u}_0^{\mathrm{T}} = [w_{01}\ \theta_{01}\ w_{02}\ \theta_{02}\ w_{03}\ \theta_{03}\ w_{04}\ \theta_{04}]^{\mathrm{T}},\\
&\mathbf{u}_f^{\mathrm{T}} = [w_{f1}\ \theta_{f1}\ w_{f2}\ \theta_{f2}\ w_{f3}\ \theta_{f3}]^{\mathrm{T}}.
\end{aligned} \tag{24}$$

For the modification structure (denoted by subscript 1) and the frame (denoted by subscript *f*), one finds the following constraint:

$$\begin{aligned}
&\mathbf{B}_1\,\mathbf{u}_1 - \mathbf{C}_{f1}\,\mathbf{u}_f = 0, \quad \mathbf{B}_1 = \mathbf{I}(4,4),\\
&\mathbf{C}_{f1} = \begin{bmatrix} 1/2 & L/8 & 1/2 & -L/8 & 0 & 0\\ -3/2L & -1/4 & 3/2L & -1/4 & 0 & 0\\ 0 & 0 & 5/32 & 3L/64 & 27/32 & -9L/64\\ 0 & 0 & -9/8L & -5/16 & 9/8L & 3/16 \end{bmatrix},\\
&\mathbf{u}_1^{\mathrm{T}} = [w_{11}\ \theta_{11}\ w_{12}\ \theta_{12}]^{\mathrm{T}},\\
&\mathbf{u}_f^{\mathrm{T}} = [w_{f1}\ \theta_{f1}\ w_{f2}\ \theta_{f2}\ w_{f3}\ \theta_{f3}]^{\mathrm{T}}.
\end{aligned} \tag{25}$$

Fig. 4 shows the accuracy comparison of the present partitioned, non-matching model vs. a monolithic beam model that combines the modification beam (see also Table 1), which shows the viability of the partitioned model with non-matching interface nodes.

4.2. A plate problem

The present SDM method detailed in Eqs. (1)–(22), labeled as *layout reorientation method*, is applied to a plate baseline structure for altering its dynamic characteristics by placing a set of modification beams. For the baseline plate, it has been found that the adoption of an area-element interface frame, i.e., the interface frame consists of four-noded rectangular elements, becomes convenient as shown in Fig. 5. The location where the displacement constraint condition is applied, is marked with circle on the interface frame. Note that the interface frame moves to accommodate the movement of the modification beam. Two plate problems are considered, a cantilevered plate and a corner-supported plate in order to illustrate the adaptiveness of the present method to accommodate different boundary conditions.

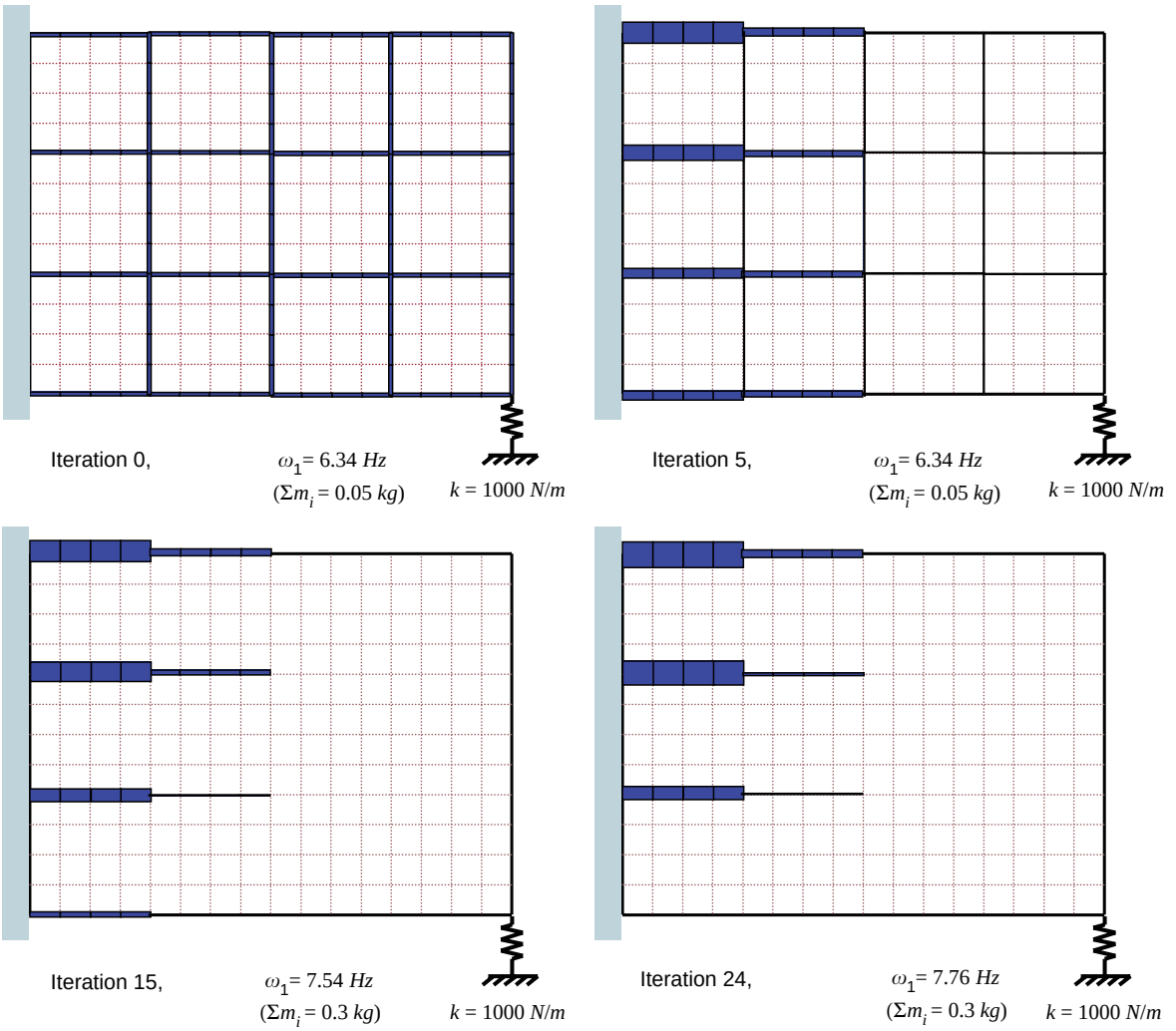

Fig. 7. Rectangular fixed layout pattern and beam width changes during optimization process (cantilevered plate).

4.2.1. A cantilevered plate

The plate baseline structure is made of steel having dimensions 600 mm by 450 mm by 2 mm as shown in Fig. 6. The plate is clamped at the left side and connected to lumped stiffness $k = 1000$ Nm at its right corner for asymmetry.

First, the 28 beams are placed in a predetermined rectangular grid pattern, labeled as *fixed layout pattern method*, is shown in Fig. 7. The optimization was carried out by changing the modification beam masses of the 28 beams and by gradually increasing the total beam mass limit. It was determined that at the end of 24 optimization iterations, no further increase in the first-mode frequency was possible as illustrated in Fig. 8. Hence, it was concluded that the optimization has converged with 7.76 Hz for the first

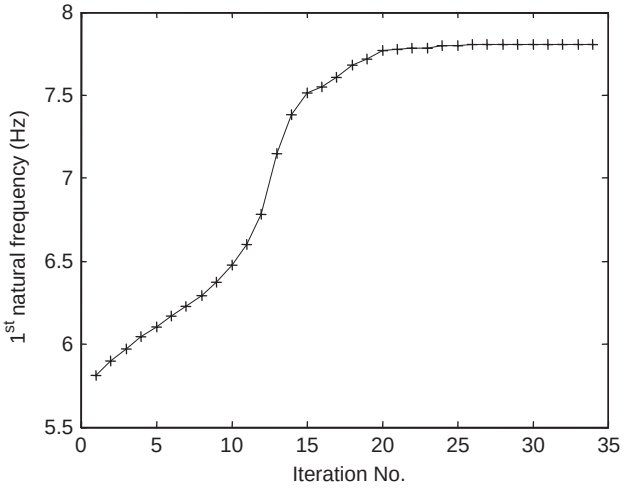

Fig. 8. Convergence of rectangular layout pattern for first-mode optimization (cantilevered plate).

mode. For curiosity, the diagonal pattern was used, which led to a lower maximum first mode (7.24 Hz) than of the rectangular pattern as shown in Fig. 9.

The same problem was tackled by the present layout reorientation method with the modification beams ranging from one to five. Each of the modification beams is chosen to be 150 mm long, 5 mm high and 10 mm wide and modeled with 4 Euler–Bernoulli beam elements. Both the plate and the beam have their modulus of elasticity of 200 Gpa and density of 7800 kg/m^3, respectively. The design variables for this problem are the location and orientation ($g_i = [x_i, y_i, \theta_i]$) for each of the modification beams. The eigenvalue sensitivity with respect to the design variables has been computed by using Eq. (22).

The optimization results for determining the beam orientation and position are shown for the case of one modification beam in Fig. 10 and for five modification beams in Fig. 11, respectively. It is found that the modification beams move from the right side to the left side in order to increase the first natural frequency of the modified plate. Although not reported herein, the cases of two to four modification beams have been examined, which are summarized in Table 2. Clearly, the fundamental frequency increases as the number of the modification beams is increased while keeping the total mass of the modification beams is constrained to be the same as for the fixed layout pattern case. Specifically, when one employs five modification beams, the fundamental frequency attained exceeds that obtained by the fixed-pattern case. This demonstrates the flexibility and potential of the present structural modification method as no a priori assumption is needed for their final orientations.

To compare and contrast to the fixed layout pattern method, the same plate structural modification problem was rerun using the present layout reorientation method, with five 135° inclined initial modification beams as opposed to five horizontal modification beams considered in Fig. 11. The result is illustrated in Fig. 12, which indicates that the final modification pattern is qualitatively the same as the case of Fig. 11. In other words, the present layout reorientation method is somewhat insensitive to initial layout of modification structures, an important advantage over the fixed layout pattern method.

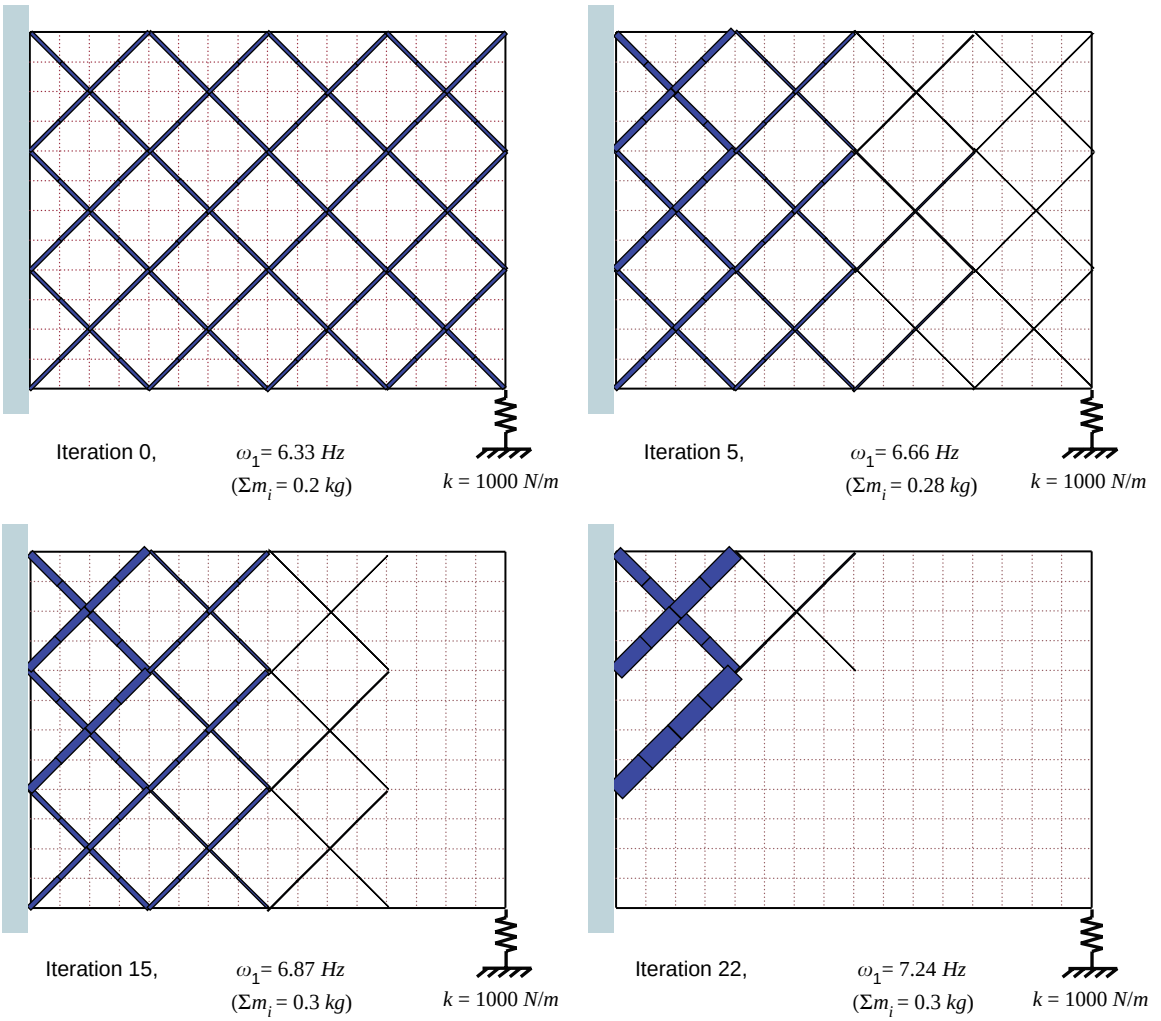

Fig. 9. Cross fixed layout pattern and beam width changes during optimization process (cantilevered plate).

4.2.2. A two-corner supported plate

The same plate is used for two-corner supported boundary conditions as shown in Fig. 13. The optimization results of the fixed layout pattern method are illustrated in Figs. 14 and 15 for two different patterns. Clearly, the diagonal pattern yields somewhat higher fundamental frequency than that of the horizontal pattern. This shows that a desirable initial pattern is influenced by the different boundary conditions.

As for the present layout reorientation method with one to five beam elements, Table 3 shows that the present layout reorientation method with three modification beam elements yields a competitive fundamental frequency compared to the fixed layout pattern method. In addition, the same plate modification problem was rerun using the present layout reorientation method with a diagonal initial orientation pattern of the modification beams. The results are summarized in Figs. 16 and 17, which illustrate that the

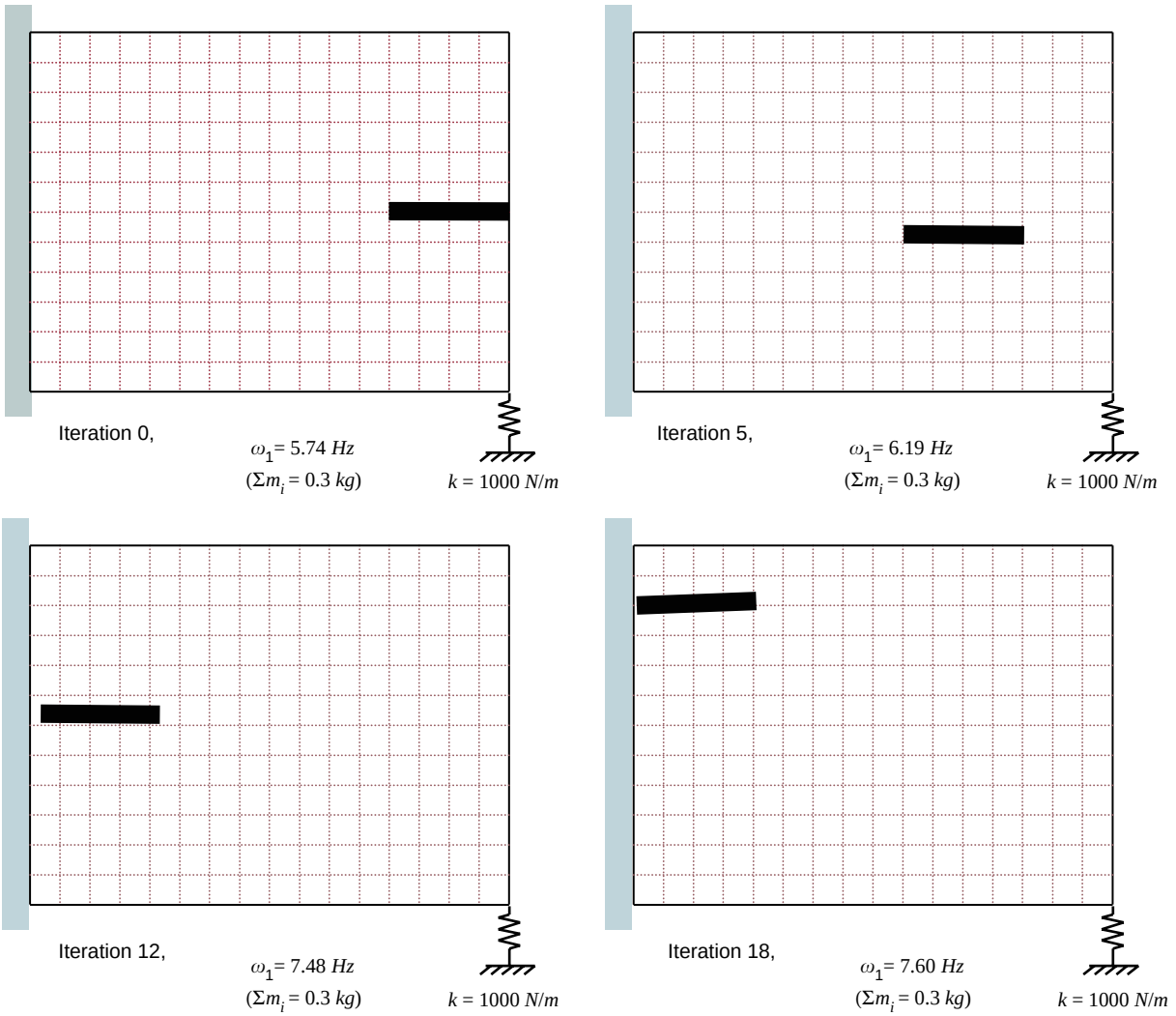

Fig. 10. Present layout reorientations of a beam stiffener during optimization process (cantilevered plate).

final layout of modification beams converges to that of the fixed layout pattern method with the diagonal pattern (see Fig. 15). A major difference is that, whereas the final result by the fixed layout pattern method forms two diagonal beams, that of the present layout reorientation method forms only one beam line.

It is observed that, for the example problems considered, different fixed patterns influence more significantly the final optimization results (4% for the present example) of the fixed layout pattern method than those of the present layout reorientation method (less than 1%). This illustrates that, even for problems that may yield different modification layout depending on the initial layout, the present layout reorientation method yields almost the same achievable frequency levels. This is not the case with the fixed layout pattern method.

Finally, for the three problems evaluated, the present layout reorientation method is more efficient than the fixed layout pattern method.

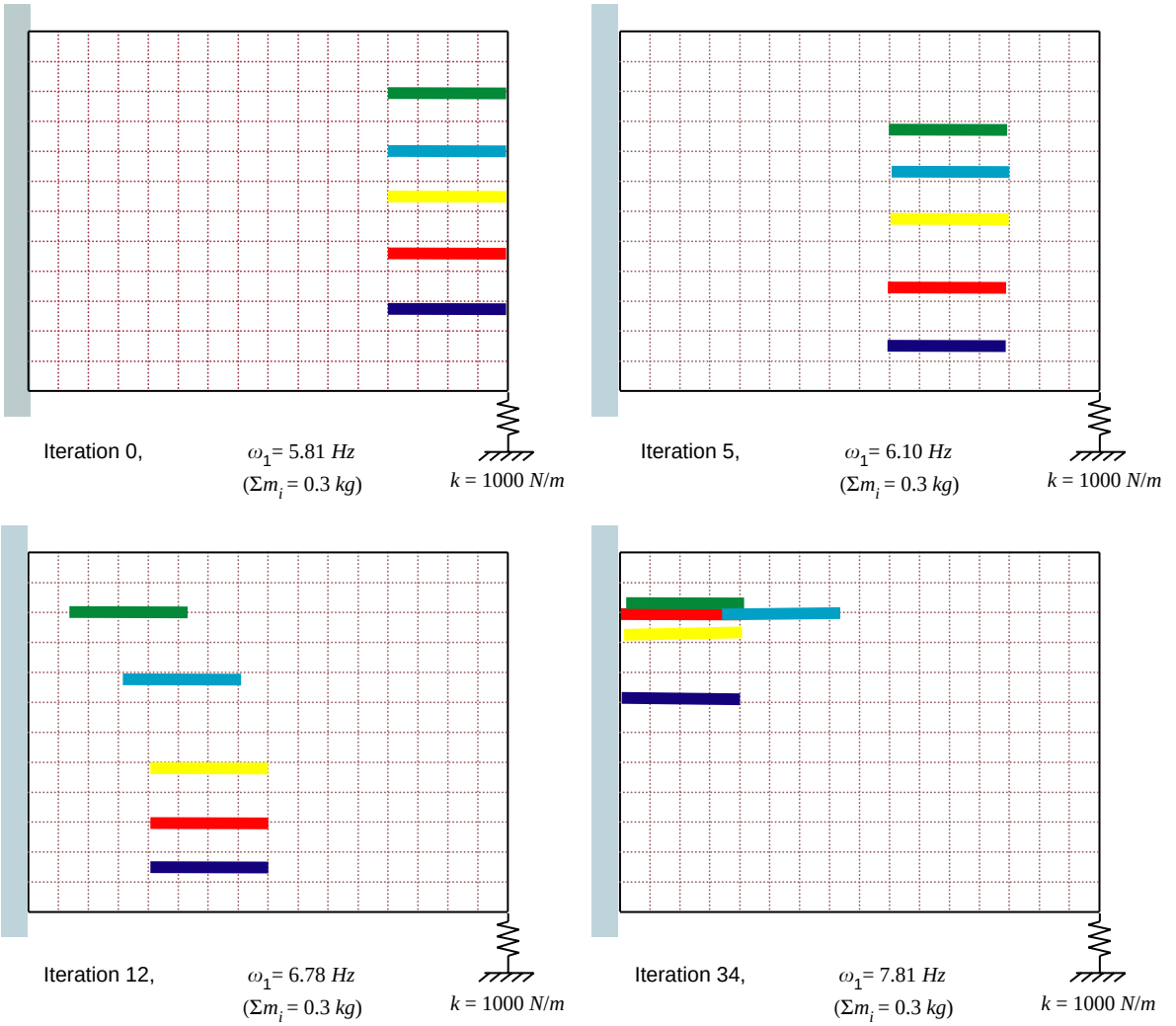

Fig. 11. Present layout reorientations of initially horizontal five beam stiffeners during optimization process (cantilevered plate).

Table 2
Comparison of fixed layout pattern vs. present layout reorientation methods for cantilevered plate

Baseline plate	Size optimization	Position optimization				
		1 beams	2 beams	3 beams	4 beams	5 beams
6.21 Hz	7.76 Hz	7.60 Hz	7.67 Hz	7.68 Hz	7.80 Hz	7.81 Hz

Maximum adding mass: 0.3 kg.

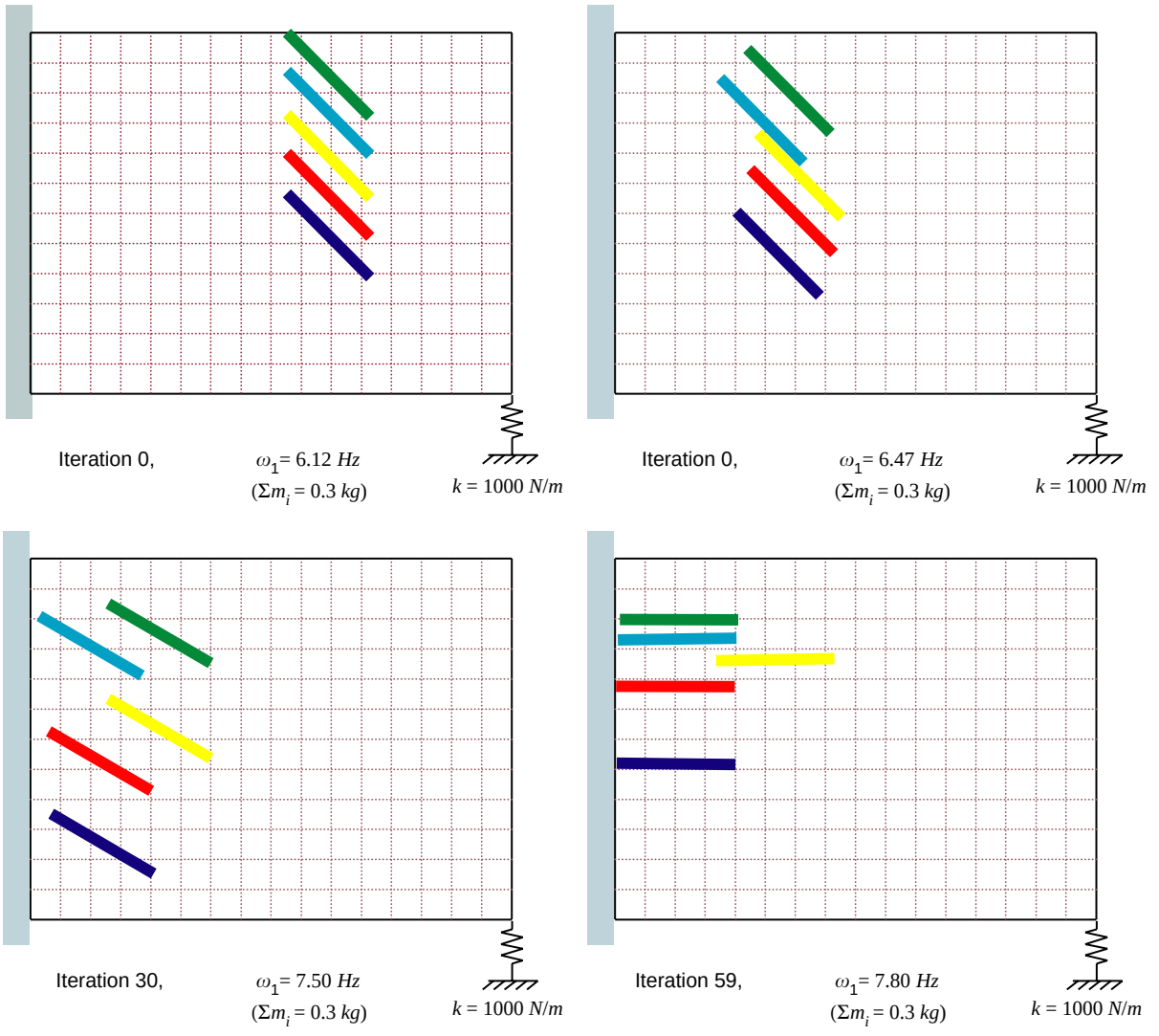

Fig. 12. Present layout reorientations of initially diagonal five beam stiffeners during optimization process (cantilevered plate).

5. Conclusion

In this work, position changes and reorientation of modification structures are utilized as the design optimization variables for improving the frequencies and/or mode shapes of the baseline structure. The partitioned equations of motion are used to model independently the baseline structure and the modification substructures, and a frame concept is introduced to address the coupling of non-matching interface nodes. Computations of the natural frequencies of the combined structure are carried out by the resulting interface FRFs, thus reducing the number of degrees of freedom in eigenvalue problem as the number of interface degree of freedom usually substantially smaller than the total degrees of freedom of the baseline structure and the modification substructures. An eigenvalue sensitivity in terms of the optimization variables, viz.,

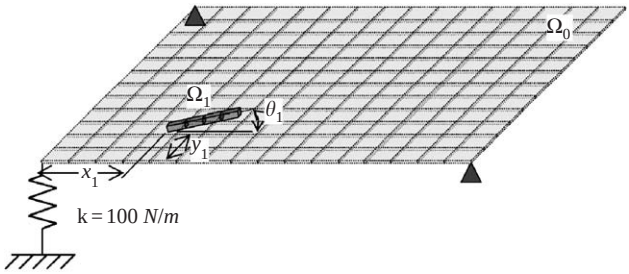

Fig. 13. Diagonally corner-supported plate.

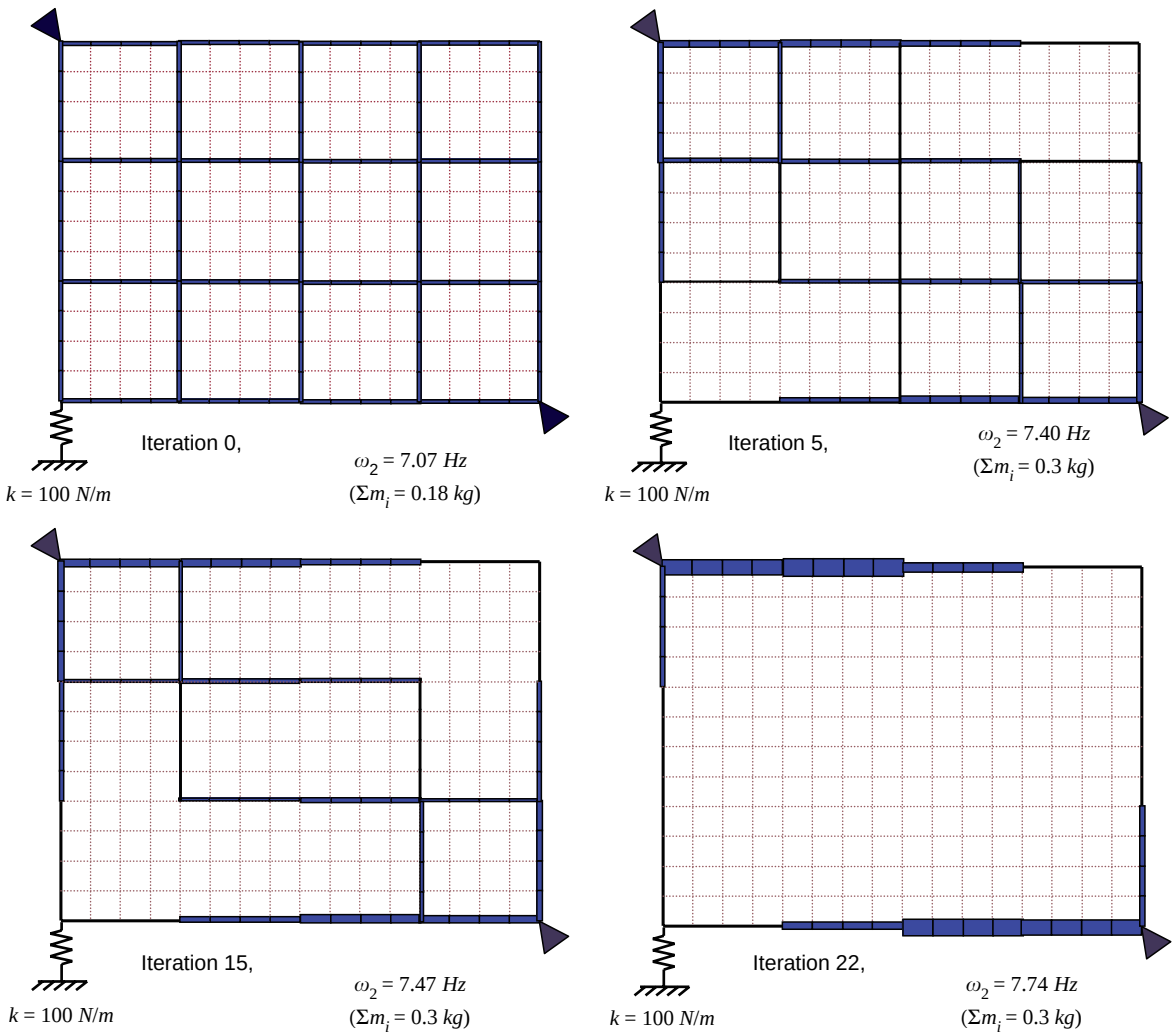

Fig. 14. Rectangular fixed layout pattern and beam width changes during optimization process (corner-supported plate).

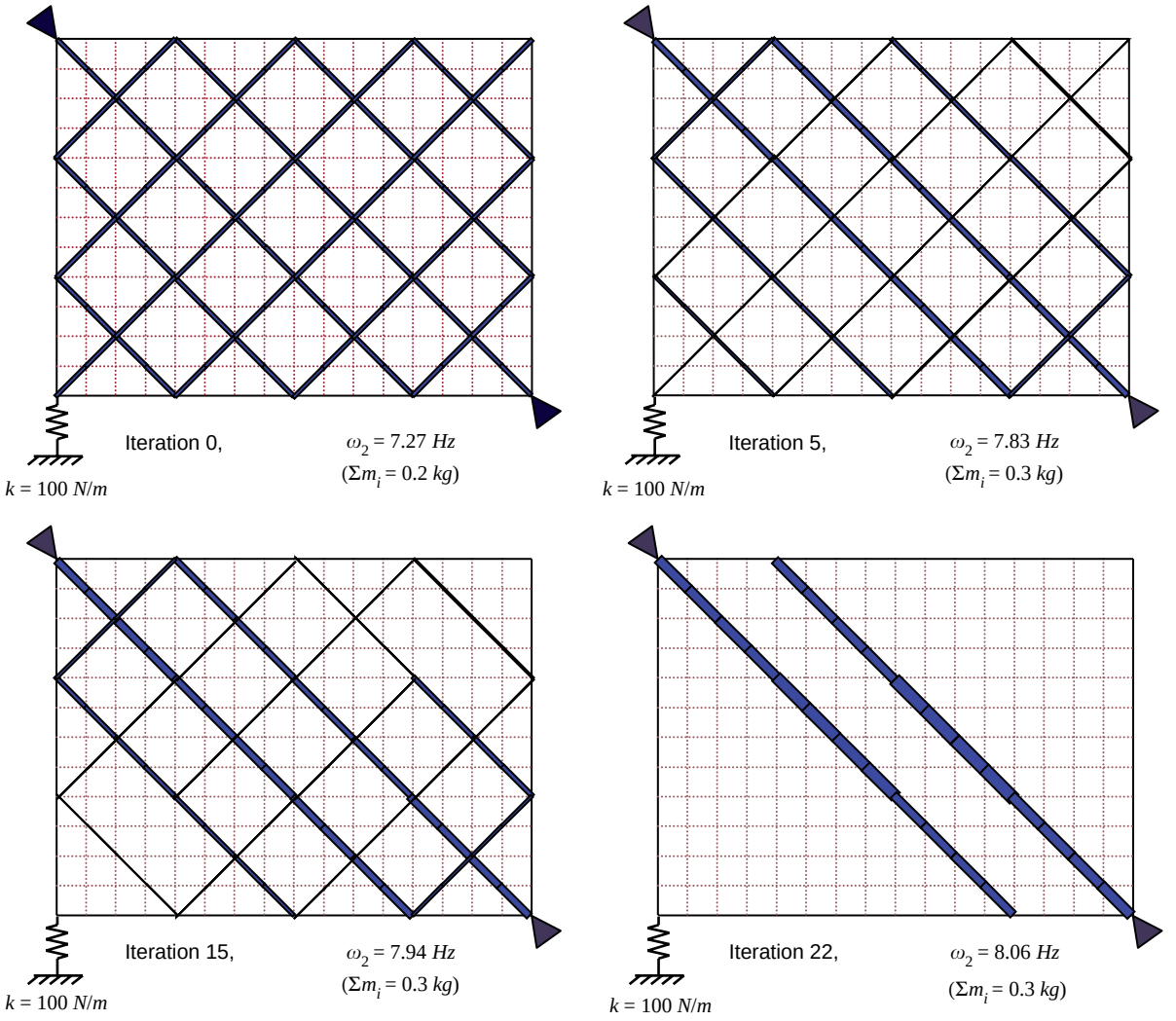

Fig. 15. Cross fixed layout pattern and beam width changes during optimization process (corner-supported plate).

the position and the orientation of modification substructures, is derived and used to find the modification direction and orientation. Finally, the optimal structural modification is iteratively calculated by combining the eigenvalue sensitivities and exact eigenvalue reanalysis results. The present layout reorientation SDM method has been applied to determine the position and orientation of beam stiffeners to increase the natural frequency of the baseline plate and compared to the fixed layout pattern SDM method that employs the beam width as the design variable. The result is encouraging both in terms of its conceptual simplicity as the present method can take advantage of software modularity for large-scale SDM problems. Further studies would provide insight as to its applicable ranges and limitations, which we are actively pursuing.

Table 3
Comparison of fixed layout pattern vs. present layout reorientation methods for corner-supported plate

Baseline plate	Size optimization	Position optimization				
		1 beams	2 beams	3 beams	4 beams	5 beams
6.88 Hz	7.74 Hz	7.20 Hz	7.50 Hz	7.78 Hz	7.92 Hz	7.97 Hz

Maximum adding mass: 0.3 kg.

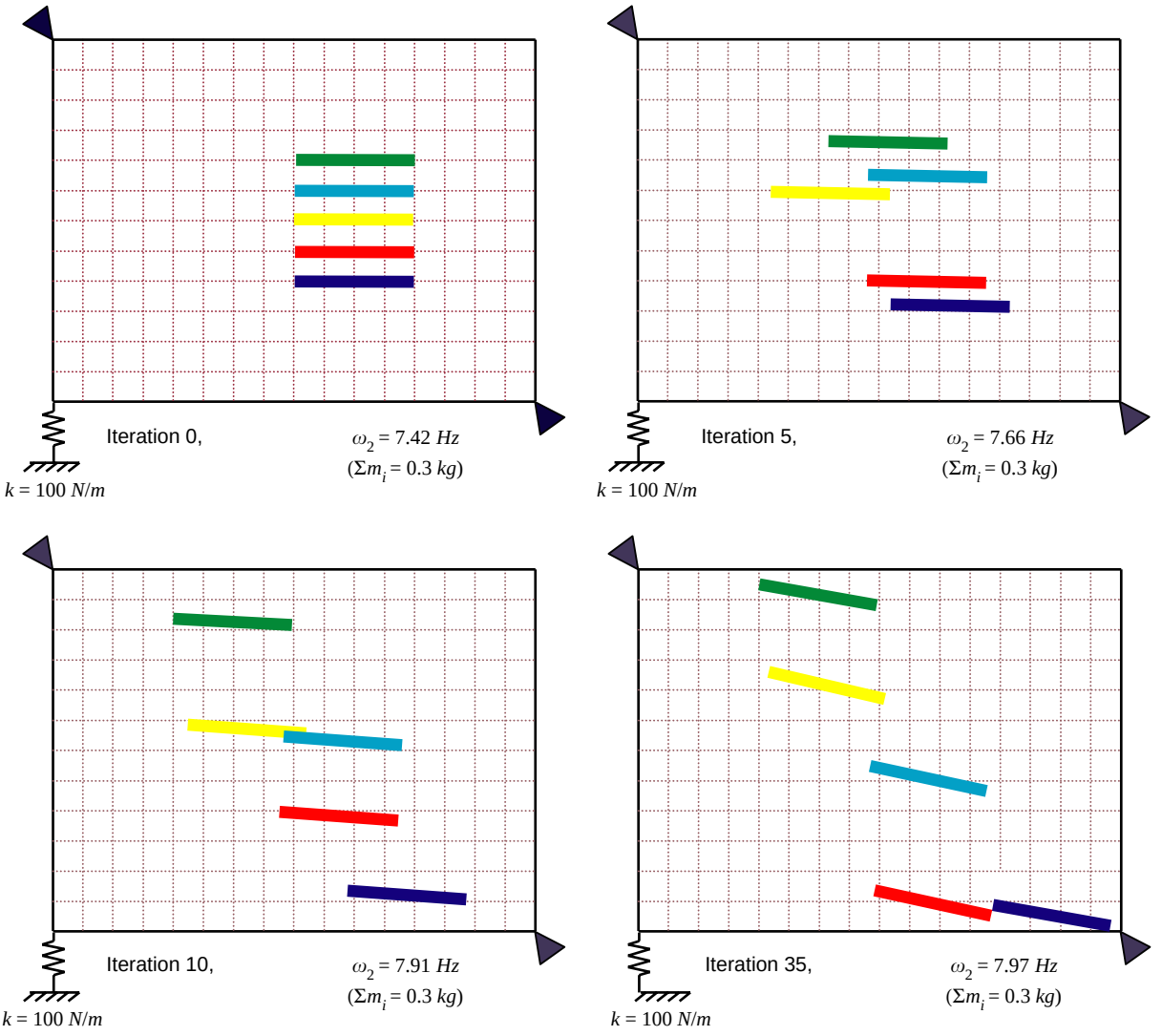

Fig. 16. Present layout reorientations of initially horizontal five beam stiffeners during optimization process (corner-supported plate).

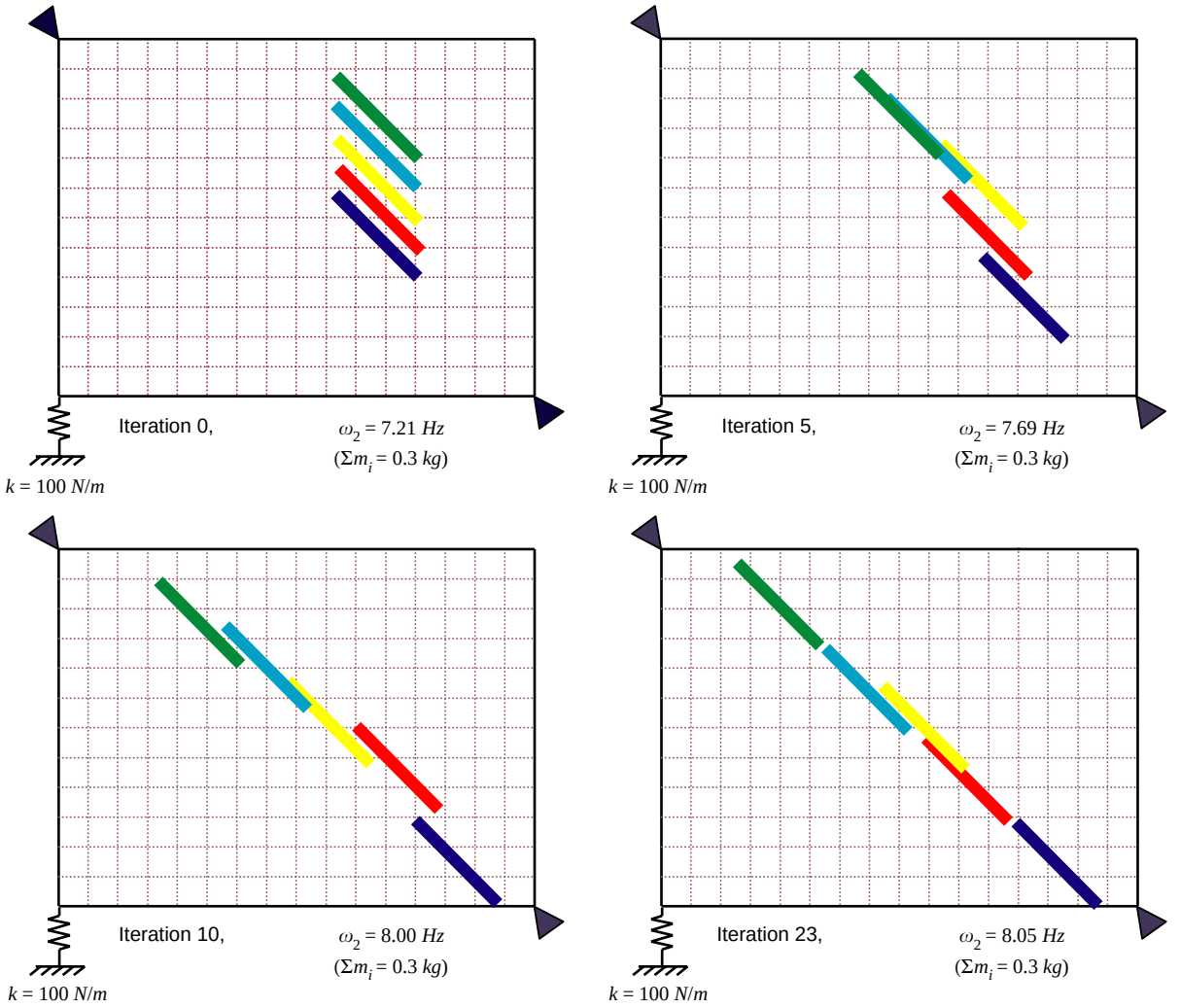

Fig. 17. Present layout reorientations of initially diagonal five beam stiffeners during optimization process (corner-supported plate).

Acknowledgements

This work was supported by the National Research Laboratory Program of Ministry of Science and Technology, Republic of Korea, Contract/grant number 2000-N-NL-01-C-148. The third author wishes to acknowledge his visiting professorship appointment at Korea Advanced Institute of Science and Technology (KAIST) during the summers of 2002–2004.

References

[1] C.J. Hoff, M.M. Bernitsas, R.E. Sandstrm, W.J. Anderson, Inverse perturbation method for structural redesign with frequency and mode shape constraints, AIAA J. 22 (9) (1984) 1304–1309.

[2] M.J. Smith, S.G. Hutton, Frequency modification using Newtons method and inverse iteration eigenvector updating, AIAA J. 30 (7) (1992) 1886–1891.
[3] M.J. Smith, S.G. Hutton, A perturbation method for inverse frequency modification of discrete, undamped systems, J. Appl. Mech. 61 (7) (1994) 887–892.
[4] M.P. Bendsøe, O. Sigmund, Topology Optimization: Theory, Methods and Applications, Springer, Berlin, 2003.
[5] A.R. Diaz, N. Kikuchi, Solution to shape and topology eigenvalue optimization problems using a homogeneous method, Internat. J. Numer. Methods Eng. 35 (1992) 1487–1502.
[6] A.S. Lewis, M.L. Overton, Eigenvalue optimization, Acta Numerica 5 (1996) 149–190.
[7] Sung-Ling Twu, Kyung K. Choi, Configuration design sensitivity analysis of built-up structures Part I: theory, Internat. J. Numer. Methods Eng. 35 (1992) 1127–1150.
[8] Sung-Ling Twu, Kyung K. Choi, Configuration design sensitivity analysis of built-up structures Part II: numerical method, Internat. J. Numer. Methods Eng. 36 (1993) 4201–4222.
[9] C. Farhat, M. Geradin, On a component mode synthesis method and its application to incompatible substructures, Comput. Struct. 51 (5) (1994) 459–473.
[10] K.C. Park, C.A. Felippa, A variational principle for the formulation of partitioned structural systems, Internat. J. Numer. Methods Eng. 47 (2000) 395–418.
[11] K.C. Park, C.A. Felippa, Rebel, A simple algorithm for localized construction of non-matching structural interface, Internat. J. Numer. Methods Eng. 53 (2002) 2117–2142.
[12] Jen-Yi Liao, Chuan-Cheung Tse, An algebraic approach for the modal analysis of synthesized structures, Mech. Systems Signal Process. 7 (1) (1993) 89–104.
[13] E.K.L. Yee, Y.G. Tsuei, Direct component modal synthesis technique for system dynamic analysis, AIAA J. 27 (8) (1989) 1083–1088.
[14] A. Simpson, The Krons methodology and practical algorithms for eigenvalue, sensitivity and response analysis of large scale structural systems, Aeronaut. J. 84 (1980) 417–433.
[15] Yong-Hwa Park, Youn-Sik Park, Structure optimization to enhance its natural frequencies based on measured frequency response functions, J. Sound Vibration 229 (5) (2000) 1235–1255.